Repeatable ecological dynamics govern the response of experimental communities to antibiotic pulse perturbation

Cairns, Johannes

2020-10

acceptedVersion

1
2
1. Extended Data

4

Figure #	Figure title One sentence only	Filename This should be the name the file is saved as when it is uploaded to our system. Please include the file extension. i.e.: *Smith_ED Fig1.jpg*	Figure Legend If you are citing a reference for the first time in these legends, please include all new references in the Online Methods References section, and carry on the numbering from the main References section of the paper.
Extended Data Fig. 1	Extended Data Fig. 1	Fig_S1.tiff	**Figure S1.** A t-SNE map showing *de novo* community clustering before, during and after recovery from antibiotic pulse at different antibiotic levels with or without immigration (N = 190). The different antibiotic levels are indicated by color coding, and the time points relative to the antibiotic pulse are indicated by different shapes. Low, intermediate and high antibiotic levels correspond to 4, 16 and 128 μg ml^{-1} streptomycin, respectively. All data points originate from the same t-SNE analysis and have been separated into two panels (with same arbitrary axis units) only for the sake of visual clarity of immigration effect (at high antibiotic level, post-recovery communities indicated by diamonds more often resume pre-disturbance composition in upper left-hand region).
Extended Data Fig. 2	Extended Data Fig. 2	Fig_S2.tiff	**Figure S2.** The extinction probability of species as a function of antibiotic level and the presence/absence of immigration (binomial glm estimate ± 95 % confidence intervals). Extinction is defined as the absence of a species after the antibiotic pulse (day 32 onwards) that was present prior to the pulse (day 16), and has been computed only for the species fulfilling these criteria in at least one experimental community (in total, 146 cases of

			extinction were observed). Low, intermediate and high antibiotic levels correspond to 4, 16 and 128 μg ml^{-1} streptomycin, respectively.
Extended Data Fig. 3	Extended Data Fig. 3	Fig_S3.tiff	**Figure S3.** Bacterial biomass estimated by optical density (OD) at 600 nm at different levels of antibiotic pulse (expressed in μg ml^{-1}) in the pre-disturbance (day 16), post-disturbance (day 32) and post-recovery (day 48) phases (mean ± standard deviation).
Extended Data Fig. 4	Extended Data Fig. 4	Fig_S4.tiff	**Figure S4.** Global comparative view of community composition as shown by Kullback-Leibler (KL) divergence across all samples (N = 190). The color scale from blue to red indicates the degree to which community composition differs between two communities. KL divergence has been computed from species compositional data. The heat map has been color-annotated for the different immigration and antibiotic treatments and experimental phases. Low, intermediate and high antibiotic levels correspond to 4, 16 and 128 μg ml^{-1} streptomycin, respectively.
Extended Data Fig. 5	Extended Data Fig. 5	Fig_S5.tiff	**Figure S5.** Competitive fitness landscapes across all samples during the antibiotic pulse and recovery phases (N = 126). The color scale from blue to red indicates the degree to which the competitive fitness landscapes are correlated between two communities. Correlations have been computed from competitive fitness data for each species in the communities. The heat map has been color-annotated for the different immigration and antibiotic treatments and experimental phases. Low, intermediate and high antibiotic levels correspond to 4, 16 and 128 μg ml^{-1} streptomycin, respectively. The black boxes show the data presented at species-level detail in Figure 4 in the main text.
Extended Data Fig. 6	Extended Data Fig. 6	Fig_S6.tiff	**Figure S6.** Correlation of competitive fitness landscapes

			within replicates in each experimental treatment (mean + 95 % confidence interval). Correlations have been computed from competitive fitness data for each species in the communities. The figure aggregates the pairwise correlation values shown for each replicate pair within treatments in Figure S4. Low, intermediate and high antibiotic levels correspond to 4, 16 and 128 μg ml^{-1} streptomycin, respectively.
Extended Data Fig. 7	Extended Data Fig. 7	Fig_S7.tiff	**Figure S7.** Percentage of variance in the competitive fitness of species explained by the experimental treatments (antibiotic level and presence / absence of species immigration) and species traits (antibiotic MIC and intrinsic growth rate). The variance partitioning is based on ANOVA on competitive fitness performed separately for the antibiotic pulse and recovery phases (detailed results are presented in Tables S1 and S2).
Extended Data Fig. 8	Extended Data Fig. 8	Fig_S8.tiff	**Figure S8.** Illumina read recruitment (median per species) in whole genome alignments for deep sequencing data (two upper panels) or raw 16S rRNA amplicon data (bottom panel). The HAMBI codes of the species are indicated in the horizontal axis, with two exceptions: K12 and RP4 denote the chromosome and plasmid sequence, respectively, from *E. coli* JE2571. Read recruitment in whole genome alignments is indicated as number of reads (100 bp) in 1,000 bp blocks, and needs to be divided by 10 ((100 bp × read count)/(1,000 bp block)) to obtain an estimate of genome coverage. For instance, a median read count of 1,000 corresponds to roughly 100× genome coverage. In the uppermost panel, deep sequencing data was mapped separately to the genome of each individual species, and in the middle panel, the data was mapped to a multi-FASTA file containing all the genomes, producing comparable results. 16S rRNA amplicon read

			counts have been normalized to 15,000 reads per sample.
Extended Data Fig. 9	Extended Data Fig. 9	Fig_S9.tiff	**Figure S9.** Deep sequencing read recruitment across the genomes of abundant species. Genomic position is indicated as relative position (0–1) across the whole chromosome for closed genomes or largest contig for draft genomes. Read recruitment in whole genome alignments is indicated as number of reads (100 bp) in 1,000 bp blocks, and needs to be divided by 10 ((100 bp × read count)/(1,000 bp block)) to obtain an estimate of genome coverage.

2. Supplementary Information:

A. Flat Files

Item	Present?	Filename This should be the name the file is saved as when it is uploaded to our system, and should include the file extension. The extension must be .pdf	A brief, numerical description of file contents. i.e.: *Supplementary Figures 1-4, Supplementary Discussion, and Supplementary Tables 1-4.*
Supplementary Information	Yes	SI.pdf	Supplementary Tables S1 to S2
Reporting Summary	Yes	nr-reporting-summary.pdf	
Peer Review Information	Yes	PRFile_Cairns.pdf	

8 Repeatable ecological dynamics govern the response of experimental com-

9 munities to antibiotic pulse perturbation

10 Johannes Cairns[1,2,3*†], Roosa Jokela[3,4*], Lutz Becks[5,6], Ville Mustonen[2,7], Teppo Hiltunen[3,8†]

11

12 ORCIDs: JC: 0000-0003-1329-2025; RJ: 0000-0002-4144-6573; LB: 0000-0002-3885-5253; VM:

13 0000-0002-7270-1792; TH: 0000-0001-7206-2399

14 [1]Wellcome Sanger Institute, Cambridge, CB10 1SA, UK

15 [2]Organismal and Evolutionary Biology Research Programme (OEB), Department of Computer Sci-

16 ence, 00014 University of Helsinki, Finland

17 [3]Department of Microbiology, P.O. Box 56, 00014 University of Helsinki, Finland

18 [4]Human Microbiome Research Program (HUMI), Faculty of Medicine, University of Helsinki, P.O.

19 Box 21, Haartmaninkatu 3, 00290 Helsinki, Finland

20 [5]Max Planck Institute for Evolutionary Biology, Department of Evolutionary Ecology, Community

21 Dynamics Group, August Thienemann Str. 2, 24306 Plön, Germany

22 [6]Limnological Institute University Konstanz, Aquatic Ecology and Evolution, Konstanz, Germany

23 [7]Helsinki Institute for Information Technology, Institute of Biotechnology, University of Helsinki,

24 Finland

25 [8]Department of Biology, 20014 University of Turku, Turku, Finland

26

27 [*]These authors contributed equally to this work

28

29 [†]Co-corresponding authors: Johannes Cairns (e-mail: johannes.cairns@helsinki.fi) and Teppo Hil-

30 tunen (e-mail: teppo.hiltunen@utu.fi)

31   Abstract

32

33   In an era of pervasive anthropogenic ecological disturbances, there is a pressing need to understand

34   the factors constituting community response and resilience. A detailed understanding of disturbance

35   response needs to go beyond associations and incorporate features of disturbances, species traits,

36   rapid evolution and dispersal. Multispecies microbial communities experiencing antibiotic perturba-

37   tion represent a key system with important medical dimensions. However, previous microbiome

38   studies on the theme have relied on high-throughput sequencing data from uncultured species with-

39   out the ability to explicitly account for the role of species traits and immigration. Here we serially

40   passaged a 34-species defined bacterial community through different levels of pulse antibiotic dis-

41   turbance, manipulating the presence or absence of species immigration. To understand the ecologi-

42   cal community response measured by amplicon sequencing, we combined initial trait data measured

43   for each species separately and metagenome sequencing data revealing adaptive mutations during

44   the experiment. We found that the ecological community response was highly repeatable within the

45   experimental treatments, which could be partly attributed to key species traits (antibiotic suscepti-

46   bility and growth rate). Increasing antibiotic levels were also coupled with increasing species ex-

47   tinction probability, making species immigration critical for community resilience. Moreover, we

48   could detect signals of antibiotic resistance evolution occurring within species at the same time

49   scale, leaving evolutionary changes in communities despite recovery at the species compositional

50   level. Together these observations reveal a disturbance response which appears as classic species

51   sorting but is nevertheless accompanied by rapid within-species evolution.

52

Introduction

In the Anthropocene[1] characterized by anthropogenic perturbations of environments ranging in scale from the individual organism (e.g. gut microbiota of mammal) to the global ecosystem (e.g. climate change and loss of biodiversity), it is paramount to understand factors determining biological resilience[2]. Understanding how the effects of perturbations percolate through the ecosystem is vital to better understand the risks and benefits of human driven control efforts in the restoration and conservation of populations. For instance, antibiotic treatment affects not only the pathogen population but also off-target species in the microbiota of the patient, promoting the spread of antimicrobial resistance[3]. Rational interventions require a detailed, ideally mechanistic, understanding that goes beyond associations, integrating community dynamics, species traits, environmental variables, evolutionary events and stochasticity. However, we are far from such an understanding, which has in part been attributed to the sparsity of controlled studies amidst *in vivo*, field and theoretical studies[4]. Nevertheless, recent advances in predictive modeling suggest that such an understanding is possible for certain rapidly evolving systems[5].

A notable case of interest is the response of multispecies bacterial communities to perturbations by antibiotics, pharmaceuticals and other compounds of an anthropogenic origin. Understanding this response can be critical, among others, for rational therapeutics to mitigate unwanted effects on patient health caused by changes in the gut microbiota (e.g. *Clostridioides difficile* infection[6]), management of waste water treatment to ensure the maintenance of key functionalities in bacterially driven processes[7], and redesigning of agricultural practices to maintain microbiota contributing to crop health and productivity[8].

77   Traditionally, ecological timescales have been considered shorter than evolutionary timescales,

78   causing ecological processes to drive the community response to environmental change. The com-

79   munity response to perturbation is therefore expected to be determined by selection on pre-existing

80   traits at the species level[9]. Selection may also act on the standing genetic variation within popula-

81   tions and affect the community response to perturbation[10-13]. However, the role of standing trait

82   variation at the species level in the bacterial disturbance response remains unclear, because large

83   population sizes and short generation times can render bacterial populations virtually unlimited by

84   mutation supply. This leads to the omnipresence and rapid generation of intraspecific trait variation,

85   which can play a major role in ecological dynamics[14], especially since mutations in the bacterial

86   genome can have strong effects on traits. For instance, a single point mutation in the gene *rpsL* can

87   make a bacterium over 250-fold more resistant to the antibiotic streptomycin[15]. Overall, strong evi-

88   dence has emerged in recent decades showing that rapid evolution can alter ecological dynamics in

89   communities across a range of systems, even those with lower rates of evolution compared to mi-

90   crobial systems[16]. Similarly, a community ecology context can be important for evolutionary trajec-

91   tories[17]. While there is an extensive number of studies on both the species compositional effects of

92   antibiotic perturbation on the microbiome and the genetics of antibiotic resistance evolution in indi-

93   vidual species, both aspects have rarely been analyzed together. Furthermore, high-throughput se-

94   quencing based approaches allowing the investigation of mutations in longitudinal microbiome data

95   have focused on *in vivo* and field samples where the species are uncultured and the pre-existing

96   traits of the species cannot be explicitly estimated[18]. This may hinder the ability to assess the im-

97   portance of evolution relative to species sorting in the perturbation response of communities.

98

99   Ecological resilience describes the ability of a community not only to withstand a perturbation (eco-

100   logical resistance) but also to recover from it. Studies have shown variable results concerning the

101   resilience of the human gut microbiota to antibiotic perturbations at high, clinical concentrations[19-21].

102   Effects of antibiotics that may or may not completely reverse after the perturbation include reduced

103   community stability[22] and diversity[23], which have been associated with adverse health consequenc-

104   es in patients[24,25]. However, the sparsity of longitudinal studies and the variability in time points

105   sampled since the perturbation pose challenges for comparing studies and assessing whether the

106   communities are still in a state of recovery at the time of sampling. Moreover, the conditions deter-

107   mining a particular community response remain unclear. These include factors such as the level of

108   perturbation and species immigration[26], a key feature of microbial communities and form of bacte-

109   riotherapy (e.g. probiotic supplementation after antibiotic treatment)[27]. There is also a practical need

110   to understand how the disturbance and immigration responses of bacterial communities interact. For

111   example, this information is critical for the design of minimal artificial communities to replace fecal

112   microbiota transplantation (FMT), where gut microbial communities disturbed by antibiotic pulses

113   are treated by a fecal "immigration" to restore a healthy microbiota[28].

114

115   Here we used a 34-species model bacterial community to examine the role of ecological and evolu-

116   tionary processes in the community response to different levels of pulse disturbance by the amino-

117   glycoside antibiotic streptomycin in the absence or presence of species immigration. We performed

118   a serial passage experiment, collecting amplicon data to track ecological dynamics and deep se-

119   quencing data to track evolutionary dynamics, and combined experimental data with pre-existing

120   trait data on community members (Figure 1). We found that communities responded sensitively and

121   repeatably to the different environments. This could be linked to species sorting and selection on

122   their traits (growth rate and antibiotic susceptibility) as well as an increase in the extinction proba-

123   bility of particular species at increasing antibiotic levels in the absence of immigration. Adaptive

124   mutations also occurred but could not be linked to the ecological dynamics. Despite the sensitive

125   response to the perturbation, communities were able to recover close to the initial community state

126   in all but the highest antibiotic level. However, the loss of species as a function of antibiotic level as

127 well as the occurrence of evolutionary changes within species still left persistent changes in com-

128 munities, compromising their resilience over the long term. Importantly, immigration played a key

129 role in resilience at the species level by preventing species extinctions.

130

131 Results

132

133 **Both antibiotic level and immigration strongly determine ecological resilience**

134

135 The communities were compositionally sensitive to the different antibiotic levels and the presence

136 of immigration (Figures 2 & 3; Extended Data Figure 1). Machine learning models could be trained

137 to correctly predict the antibiotic level during the antibiotic pulse from species composition data

138 (random forest, rf, model using community composition data from all treatments immediately post-

139 perturbation to classify antibiotic level: permutation test $p < 0.001$, accuracy estimated by leave-

140 one-out cross-validation, LOOCV, 0.88). However, the ability to distinguish between the antibiotic

141 levels decreased after the recovery period (rf model using community composition data from all

142 treatments immediately post-perturbation to classify antibiotic level: permutation test $p < 0.001$,

143 LOOCV accuracy 0.53). In contrast, machine learning models could correctly classify the immigra-

144 tion treatment only after the recovery period (rf model using community composition data from all

145 treatments immediately post-perturbation to classify immigration presence/absence: permutation

146 test $p = 0.19$, LOOCV accuracy 0.53; rf model for immigration post-recovery: permutation test $p <$

147 0.001, LOOCV accuracy 0.69). These results suggest that the antibiotic perturbation had a composi-

148 tional effect specific to the antibiotic level, this effect decreased with recovery, and the latter pro-

149 cess was influenced by species immigration.

150
151

152   To further investigate factors determining ecological resilience, we inspected the effect of the dis-

153   turbance on two measures of entropy. We used the Shannon diversity (information entropy incorpo-

154   rating species richness and evenness) after the disturbance and Kullback-Leibler (KL) divergence

155   (relative entropy comparing species composition) in individual communities over time after the

156   disturbance relative to the pre-disturbance state[29] (Figure 3). An analysis of this data shows that

157   diversity decreased (ANOVA for linear regression model on Shannon diversity with lowest AIC

158   value; antibiotic $F_{3,60} = 12.1$, $p < 0.001$; the immigration treatment did not have a significant effect

159   during the antibiotic pulse and was not included in the best model; Figure 3a) and community com-

160   position became increasingly altered as a function of antibiotic level during the pulse, and that im-

161   migration enhanced community recovery after the pulse (ANOVA for gls model on KL divergence

162   with lowest AIC value: antibiotic level $F_{3,118} = 19.8$, $p < 0.001$; immigration $F_{1,118} = 6.33$, $p = 0.013$;

163   recovery time $F_{1,118} = 8.31$, $p = 0.005$). Pairwise comparisons of estimated marginal means for KL

164   divergence show significant differences ($p < 0.02$) between all of the antibiotic levels except for the

165   control and lowest level.

166

167   Persistent alterations in community composition were only observed for the highest antibiotic level

168   in the absence of immigration (Figure 3b). Increasing antibiotic levels increased, however, species

169   extinction probability, which was strongly counteracted by immigration (ANOVA for binomial glm

170   model with lowest AIC value: antibiotic $\chi^2_{3,1643} = 22.3$, $p < 0.001$; immigration $\chi^2_{1,1646} = 27.3$, $p <$

171   0.001; species $\chi^2_{25,1618} = 166$, $p < 0.001$; antibiotic × immigration $\chi^2_{2,1615} = 7.52$, $p = 0.057$; Extend-

172   ed Data Figure 2). Therefore, in the absence of immigration, loss of species caused alterations in

173   community composition, and the magnitude of the effect was proportional to the magnitude of the

174   perturbation. The reported community effects of antibiotic level and immigration are unlikely to

175   have been affected by changes in total bacterial biomass, since similar levels of biomass were ob-

176   served across the experimental conditions and time points (Extended Data Figure 3). This indicates

11

177 that the relative abundance of species is here a close approximation of absolute abundance, which is

178 not always the case in microbial community studies and can have important implications for study

179 conclusions[30].

180

181 **Ecological dynamics are highly repeatable within antibiotic and immigration treat-**

182 **ments**

183

184 We next investigated whether increasing antibiotic levels are coupled with decreased repeatability[22]

185 in community trajectories, as this could be a signal of alternative stable states (including bi- and

186 multi-stability), stochastic species extinctions or adaptive *de novo* mutations. In contrast with this

187 expectation, we found relatively low levels of divergence in community states within each antibi-

188 otic and immigration treatment (Extended Data Figure 4). To further examine this result, we esti-

189 mated the competitive fitness of each species in the community during the antibiotic pulse or recov-

190 ery phase using the replicator equation from evolutionary game theory. In this approach, the fre-

191 quency change of one species over time is considered to be an outcome of its fitness reduced by the

192 average fitness of the community. We found that the competitive fitness of the species responded

193 repeatably to the different antibiotic levels, and that many of the species displaying a strong positive

194 response during the pulse displayed an inverse response during the recovery phase (intermediate

195 antibiotic level without immigration illustrated in Figure 4; for complete data for all treatments, see

196 Extended Data Figures 5 and 6). We also found that increasing antibiotic levels increased fitness

197 variance (particular species exhibited very high or low competitive fitness values), as hypothesized

198 previously[31], which is reflected by increasingly correlated competitive fitness landscapes during the

199 antibiotic pulse and becomes reversed during the recovery phase (Extended Data Figures 5 and 6).

200 We could attribute 10–13 % variation in the competitive fitness of species during the antibiotic

201 pulse and recovery phases to the interplay between antibiotic level and key species traits, intrinsic

202   antibiotic susceptibility (streptomycin MIC) and intrinsic growth rate (r_{max}; Tables S1 and S2; Ex-

203   tended Data Figure 7). For instance, two species with high growth rate combined with high antibi-

204   otic susceptibility, *Aeromonas caviae* HAMBI 1972 (MIC = 0.75 µg ml^{-1}) and *Pseudomonas chlo-*

205   *roraphis* HAMBI 1977 (MIC = 8.0 µg ml^{-1}), decreased in abundance and competitive fitness at

206   increasing antibiotic levels (Figures 2 and 4). Potential reasons for why a higher proportion of var-

207   iation in competitive fitness could not be explained by species traits despite the highly consistent

208   ecological response include the presence of important unmeasured species traits, species interac-

209   tions, or non-linear system-level behavior (e.g. dramatic community change only after particular

210   concentration reached). Such information would be useful for predictive modelling.

211

212   To more precisely inspect the low levels of community divergence observed within treatments (Ex-

213   tended Data Figure 4), we quantified the repeatability of community trajectories within each antibi-

214   otic and immigration treatment using the diversity dissimilarity index[33] which relates diversity

215   pooled over replicate communities to the mean diversity of replicate communities. This yields a

216   value between zero and one, where zero indicates that replicate communities are identical and one

217   that they are completely different. The community trajectories were highly repeatable (close to zero)

218   in the different experimental treatments when species were weighted based on their abundance,

219   although a slight (approximately 5 %) decay in repeatability was observed for the highest antibiotic

220   level during the pulse (Shannon entropy panel in Figure 5). The high repeatability suggests that rare

221   stochastic mutational events are unlikely to have been a major driver of the ecological dynamics of

222   the abundant species. However, there was a higher decay in repeatability when species were given

223   equal weight regardless of abundance, indicating that low-abundance species account for most of

224   the loss in repeatability (species richness panel in Figure 5). When combined with the finding that

225   the extinction probability of species increased as a function of antibiotic level (Extended Data Fig-

226   ure 2), these results suggest that the stochasticity introduced by antibiotic perturbation was at least

227 partially accounted for by low-abundance species being driven extinct differentially between repli-

228 cate communities. Nevertheless, a potential role for evolutionary rescue in the stochasticity of the

229 ecological dynamics of low-abundance species cannot be ruled out.

230

231 **Antibiotic resistance mutations occur despite repeatable ecological dynamics**

232

233 To investigate mutational dynamics, we deep-sequenced three of the eight replicate communities

234 during and after recovery from the antibiotic pulse. From these community metagenomes, we could

235 extract whole-genome data for abundant species with sufficient genome coverage in a particular

236 community. We focused on genes estimated to be under selection (N = 91) based on containing

237 more nonsynonymous hits in independent populations than expected by chance. Most of these

238 genes contained mutations across experimental treatments, suggesting that they represent adapta-

239 tions to the general experimental conditions rather than treatment-specific adaptations (Figure 6).

240 Nevertheless, antibiotic and immigration also significantly enriched mutations for a small subset of

241 genes even when controlling for the presence or absence of whole-genome data (and thereby, in-

242 formation for a particular mutational target) for the different species in each community meta-

243 genome (PERMANOVA for binary vectors of mutated genes, i.e. mutational profiles: species R^2 =

244 0.81, $p < 0.001$; antibiotic $R^2 = 0.015$, $p < 0.001$; immigration $R^2 = 0.0082$, $p < 0.001$).

245

246 Among the mutational targets that occurred only in the presence of the antibiotic, several have been

247 previously associated with increased levels of streptomycin or aminoglycoside resistance or with

248 the presence of these agents, suggesting that antibiotic-related adaptations occurred during the ex-

249 periment. These genes include *rpsL* (encoding ribosomal protein S12, a common streptomycin re-

250 sistance target)[34], *rsmG* (ribosomal methyltransferase)[35], *phoQ* (PhoP-PhoQ two-component regula-

251 tory system)[36], *cya* (adenylate cyclase)[37], *cra* (catabolite repressor/activator)[37], *cspA* (cold shock

14

252 protein)[38], *relA* (GTP pyrophosphokinase mediating stringent response)[15] and *spoT* ((p)ppGpp syn-

253 thase/hydrolase mediating stringent response)[15]. Most of these mutations occurred in the intermedi-

254 ate or highest antibiotic concentration, while displaying no general pattern with respect to the pres-

255 ence or absence of immigration (observed only without immigration: *rpsL* (1×) and *cspA* (2×); only

256 with immigration: *rsmG* (2×); both without and with immigration: *cra* (2×), *cya* (13×), *phoQ* (2×),

257 *relA* (4×); Figure 6). Notably, mutations in a particular gene were not required for a species to suc-

258 ceed at a given antibiotic level. For instance, an *rpsL* mutation in *Agrobacterium tumefaciens*

259 HAMBI 105 and *rsmG* mutations in *Pseudomonas chlororaphis* HAMBI 1977 only occurred in a

260 subset of the replicates where the species displayed high abundance in the respective antibiotic

261 treatment (Figure 6). The low level of within-treatment repeatability in mutational targets contrasts

262 with the high level of within-treatment repeatability in ecological trajectories for abundant species.

263 Therefore, we could not detect an influence of genomic evolution on the ecological dynamics with

264 the methods employed in this study, although we acknowledge the limitations of our approach (fo-

265 cusing on abundant species in a subset of replicates).

266

267 **Discussion**

268

269 Using a controlled setup to investigate the antibiotic response of a multispecies bacterial community

270 in the presence and absence of species immigration, we found that the replicate communities re-

271 sponded repeatably to the different treatments, with the magnitude of the community response and

272 persistent community changes increasing with increasing antibiotic levels. The community effects

273 of antibiotics expectedly included both abundance changes and extinctions of particular species.

274 Persistent community changes were linked to increasing species extinctions at increasing antibiotic

275 level, which prevented abundant high-growth-rate species sensitive to the antibiotic from rebound-

276 ing to their pre-disturbance abundance during the recovery phase, and could be counteracted by

15

277   species immigration. This was not a straightforward outcome, since the original community compo-

278   sition may not have recovered despite reintroduction of sensitive species if communities had

279   reached an alternative stable state during the antibiotic pulse. Overall, these findings highlight the

280   importance of classic and relatively simple ecological processes, species sorting and immigration,

281   in defining how microbial communities respond to antibiotic perturbation.

282

283   The high level of repeatability of the ecological dynamics in our study appears to contrast with pre-

284   vious studies showing decreased stability[22] and bistability[39] in microbial communities following

285   antibiotic exposure. However, similar to these studies, the minor decay in repeatability we observed

286   did occur under high antibiotic levels (Figure 5). Furthermore, at the intermediate antibiotic level,

287   certain replicate communities experienced a more dramatic decline in diversity compared to others

288   (Figure 3a and Extended Data Figure 1), indicating that this antibiotic level may be close to a tip-

289   ping point concentration where bistable system-level behavior is possible. Quantifying these effects

290   more precisely would have required experimenting with a wider range of antibiotic concentrations.

291   Moreover, a previous study shows that high rates of immigration can fuel adaptation to antibiotics

292   by increasing the supply of genetic variation[40]. Therefore, higher levels of immigration could poten-

293   tially have exacerbated the role of evolution in our immigration treatment such that replicate com-

294   munities would have diverged more during the antibiotic pulse, as species containing adaptive mu-

295   tations by chance or the timing of occurrence of these mutations would differ between them. This

296   could also have decreased the rate of recovery in the immigration treatment, since there would have

297   been an increased likelihood of communities reaching alternative stable states and larger differences

298   in post-disturbance genetic composition may have slowed down species compositional recovery

299   rate. However, establishing this would have required experimenting with different levels of immi-

300   gration. Therefore, the level of ecological repeatability observed may be influenced by a number of

301   study conditions.

302

We also found adaptive mutations sweeping to high frequencies in populations of individual species, although we could not connect these with species abundance. This shows that the disturbance response in microbial systems results from a combination of ecological and evolutionary processes operating at the same timescale. However, connecting these processes may not always be straight-forward[41.] Similar to our finding, in a recent analysis of longitudinal linked-read sequencing data from human gut microbiota subjected to antibiotic treatment, antibiotic resistance mutations were found to sweep to high frequencies in the populations of single species without necessarily resulting in an increased abundance of the species in the community[18]. In a microbial community, species sorting and adaptive mutations occur simultaneously in multiple species, and all these factors have the potential to interact, making it challenging to disentangle ecological from evolutionary process-es. Furthermore, in a number of conditions, relative fitness increases within a species based on al-lele frequency changes do not translate into changes in absolute fitness (population size)[32]. In a multispecies setup, the competitive release of an adapted species may be suppressed, for example, by the presence of other abundant species with relatively low intrinsic antibiotic susceptibility and equal or higher resource use ability. The occurrence of a fitness trade-off between growth rate and antibiotic resistance[42] could also make the net fitness advantage of antibiotic resistance low, causing a weak ecological effect difficult to detect in a multispecies setup. Importantly, whatever the under-lying mechanism, this study supports the notion that within-species adaptive evolution can occur during a perturbation even when this is not readily suggested by the ecological dynamics.

322

Our findings have important implications for the understanding and management of ecological re-silience. Although we found similar outcomes from antibiotic perturbation as those reported in hu-man gut microbiome studies, such as decreased diversity[23], these outcomes were mostly limited to the community state at the end of the perturbation, and were followed by community recovery close

327   to the pre-disturbance state. This is non-trivial taken that priority effects[43] or the presence of alter-

328   native stable states[44,45] could cause a perturbed community to recover to an altered state, and em-

329   phasizes the need to assess ecological resistance during perturbations separately from recovery and

330   longer-term resilience[46]. More generally, since the advent of amplicon and metagenomic sequenc-

331   ing, changes in bacterial communities have been found in response to a plethora of environmental

332   factors, but our findings suggest that such changes may not persist and a need for caution in data

333   interpretation in the absence of longitudinal data. Nevertheless, despite the communities mostly

334   rebounding, species extinctions, which were more likely at increasing antibiotic levels, left persis-

335   tent marks in community composition, similar to recent findings from human gut microbiota[20], alt-

336   hough species immigration enabled community recovery. This indicates that storing and reintroduc-

337   ing susceptible low-abundance species with key functionalities could play a crucial role in human

338   management of ecological disturbances. Ecological resilience was most notably compromised for

339   the highest antibiotic level, suggesting that in a therapeutic context, intermediate antibiotic levels

340   may represent a desirable compromise minimizing off-target effects assuming they are sufficient to

341   treat a pathogen[3]. Notably, here we considered only a single pulse disturbance, while communities

342   often face multiple disturbances, with historical disturbance regimes frequently priming populations,

343   communities and ecosystems, both ecologically and evolutionarily, to similar disturbances in the

344   future[39,47,48]. Therefore, the types of persistent ecological (lost species) and evolutionary (resistance

345   mutations) changes observed in this study may have important consequences for the response of

346   communities to future perturbations.

347

348   Methods

349

350   **Strains and culture conditions**

351

18

352 The liquid medium used in the experiment was specifically developed for complex communities

353 and a long culture cycle. An artificial bacterial community consisting of 34 species (for species list,

354 see Supplementary Materials in [49]) was almost entirely chosen from the HAMBI Culture Collection,

355 University of Helsinki, except for *Escherichia coli* K-12 strain JE2571[50]. The bacteria are gram-

356 negative and represent three classes (Alpha-, Beta- and Gammaproteobacteria) in the phylum Prote-

357 obacteria and three classes (Chitinophagia, Flavobacteriia and Sphingobacteriia) in the phylum Bac-

358 teroidetes. The species are not representative of a particular natural system but were rather selected

359 based on growth in simple, uniform laboratory conditions. Different versions of the artificial com-

360 munity have been used in two previous studies[49,51], where details are reported regarding its con-

361 struction and the phenotypic and genomic characteristics of the species.

362

363 A medium was specifically refined for the selected community and long culture cycles. The co-

364 culture medium contains 1 g l^{-1} R2A broth (Labema, Helsinki, Finland) and 0.5 g l^{-1} of cereal grass

365 medium (Ward's Science, St Catharines, ON, Canada) in M9 salt solution. The cereal grass medium

366 stock was prepared by autoclaving it in deionized H_2O and filtering through 5 μl to remove particu-

367 late matter.

368

369 **Serial passage experiment**

370

371 A 48-day serial passage antibiotic pulse experiment was performed consisting of three epochs: 16

372 days without streptomycin to allow the community composition to acclimatize to experimental con-

373 ditions, 16 days with streptomycin at the concentrations 4, 16, and 128 μg ml^{-1}, and 16 days without

374 antibiotics to allow the community to recover (Figure 1). The experiment included an antibiotic-free

375 control treatment. The experiment was performed in a full-factorial design without and with immi-

376 gration consisting of adding an inoculum of the original community at each transfer. Each treatment

377 combination was replicated eight times.

378

379 The experiment was conducted in ABgene™ 96 Well 2.2 ml Polypropylene Deepwell Storage

380 Plates (Thermo Fisher Scientific, Waltham, MA, USA) in the co-culture medium. Prior to starting

381 the experiment, all the strains were transferred to the co-culture medium and cultured for 96 hours

382 at 28 °C / 50 rpm. Following this, they were pooled together in equal volumes and freeze-stored

383 with 30% glycerol at –80 °C. To start the experiment, 10 μl of 100-fold diluted freezer-stock com-

384 munity was added to each well containing 500 μl of medium and 50 μl of sterile dH_2O to compen-

385 sate the dilution caused by streptomycin additions. Equal volumes were used instead of using more

386 precise methods such as plate counting or flow cytometry to equalize cell numbers for each species

387 prior to starting the experiment since we assumed that uncertainty in the latter methods and differ-

388 ences between species in cell viability and revival from frozen inoculum would nevertheless have

389 introduced substantial initial differences in species abundances. We therefore accepted that the

390 starting conditions are biased toward high growth ability species which would in any case have

391 been likely to rise to dominance rapidly during the initial culture cycles (first 16-day acclimation

392 epoch). Culturing throughout the experiment was performed at 28 °C / 50 rpm. The experiment was

393 maintained every 96 hours by transferring 50 μl, about 10%, to fresh medium prepared as in the

394 beginning of the experiment (representing approx. 3.33 bacterial generations per culture cycle with

395 the minimal assumption that bacteria multiply until reaching carrying capacity). For the immigra-

396 tion treatment, 10 μl of 100-fold diluted freeze-stored community was also added. For cultures con-

397 taining streptomycin, the dH_2O was replaced with an equal volume of the appropriate streptomycin

398 stock solution.

399

400 **Data collection**

401

402   The pre-existing phenotypic trait data for community members used in this study, including intrin-

403   sic growth rate and streptomycin minimum inhibitory concentration (MIC) values, was obtained as

404   described previously[49]. To monitor bacterial density during the serial passage experiment, optical

405   density values at 600 nm wavelength (OD_{600nm}) were measured from old cultures prior to the dis-

406   turbance (day 16), after the disturbance (day 32), and after the recovery period (day 48) using a well

407   plate reader (Tecan Infinite M200 well-plate reader, Tecan Trading AG, Switzerland). Samples

408   from time points 16 days (before streptomycin addition), 32 days (last time point with streptomycin)

409   and 48 (final time point) days were also frozen in glycerol at –80 °C for further analysis.

410

411   DNA was extracted from the original freezer-stock community and the first three (1–3) out of eight

412   experimental replicate communities from days 16, 32 and 48 in the serial passage experiment for a

413   first batch of amplicon sequencing and the deep sequencing. A second batch of DNA extraction and

414   amplicon sequencing was later performed for the remaining five replicates (4–8). DNA extraction

415   was performed directly on freeze-stored samples without regrowing with the DNeasy 96 Blood &

416   Tissue Kit (Qiagen, Hilden, Germany) according to the manufacturer's instructions using 400–600

417   μl of defrosted sample. DNA concentrations were measured with the Qubit™ 2.0 (Life Technologies

418   Corporation, Carlsbad, CA, USA) fluorometer using the Qubit™ dsDNA HS Assay Kit (Thermo

419   Fisher Scientific, Waltham, MA, USA). Paired-end 16S rRNA amplicon sequencing (V3 and V4

420   regions, 2 × 300 bp; all three time points) and metagenomic deep sequencing (2 × 101 bp; only days

421   32 and 48) was performed by the Institute for Molecular Medicine Finland (FIMM) using the Illu-

422   mina MiSeq and Illumina HiSeq2500 platforms, respectively, employing in-house protocols similar

423   to those described before[49].

424

425   **Sequence data processing**

426

For 16S rRNA amplicon data, raw reads were first paired using the paired-end read merger Pear v0.9.6[52] with defaults settings. Adapters and primers were removed from the paired reads using Cutadapt v1.10[53] with the options -q 28 (quality-cutoff for trimming 3′ end of read), -n 2 (two rounds of adapter searching), -e 0.2 (maximum error rate of 20 % for adapter identification), and --minimum-length 400 (discarding reads < 400 bp after quality control steps). Read quality was controlled with FastQC v0.11.8 (www.bioinformatics.babraham.ac.uk/projects/fastqc) and MultiQC v1.7[54] before and after running Pear and Cutadapt. USEARCH v1.10[55] was used to quality filter the reads using the --fastq-filter command with the options -fastq_maxee 1 (maximum expected errors 1), -fastq_truncqual 10 (truncating reads at first incidence of quality 10), -fastq_minlen 150 (minimum read length after other filtration steps), and -fastq_trunclen 150 (truncating reads at length 150 bp). Unique sequences were obtained by dereplicating using the VSEARCH v2.13.3[56] command --derep_fulllength, followed by removal of chimeric sequences using the VSEARCH command --uchime_denovo with default settings. The reads were mapped to a reference database containing the 16S rRNA gene sequences of the 34 experimental species with USEARCH -closed_ref command with > 97 % identity requirement. Problems associated with closed reference operational taxonomic unit (OTU) clustering for environmental bacterial communities[57], such as false positive genus assignment, should not apply to this case as the community is defined and has its own reference database. The two DNA extraction and amplicon sequencing batches (replicates 1–3 vs. replicates 4–8) display a minor but distinct batch effect in community composition (Figure 2). However, performing downstream analyses separately for the two batches did not affect the qualitative findings in the study.

448

For deep sequencing data, Cutadapt 1.12[53] was used to remove sequencing adapters and quality trim sequence data, with the parameters -O 10 (minimum overlap for an adapter match), -q 28 (quality

451 cutoff for the 3′ end of each read), and --minimum-length 30 (minimum length of trimmed read).

452 Sequence data quality before and after Cutadapt was assessed using FastQC

453 (www.bioinformatics.babraham.ac.uk/projects/fastqc) and MultiQC[54]. The deep sequencing data

454 was mapped to a multi-FASTA file containing the whole-genome sequences of all experimental

455 isolates (genome accessions indicated in [49]) except for one rare species lacking genome data (*Rose-*

456 *omonas gilardii* HAMBI 2470), using bowtie2[58] with default settings. The Picard command Mark-

457 Duplicates was used to mark duplicates in alignment (BAM) files after sorting with SAMtools[59].

458 Subsequently, BEDtools 2.2 was used to compute genome coverage in 1 kb windows[60]. This pan-

459 genome mapping approach produced similar results compared to mapping the data to each genome

460 individually, indicating that genome coverage was not reduced due to biased read recruitment in

461 homologous regions, as well as cross-validating amplicon data (Extended Data Figure 8). Genome

462 coverage data also indicated a lack of major copy number aberrations (Extended Data Figure 9).

463

464 Prior to variant calling and annotation, the metagenomic alignment files were split by species using

465 SAMtools[59]. Alignment files containing below 200,000 reads, representing 5× genome coverage for

466 a 4 Mb bacterial genome, were removed. Since differential genome coverage would affect variant

467 count, nucleotide diversity and allele frequency estimates and thereby act as a confounder in down-

468 stream analyses comparing experimental treatments, all remaining BAM files were downsampled to

469 200,000 reads. Following this, genomic variants (SNPs and short INDELs) were called from BAM

470 files with FreeBayes 1.1.0-60[61], using a population level approach (--pooled-continuous) and call-

471 ing only one variant allele per locus (--use-best-n-alleles 1). Variants were filtered based on exceed-

472 ing Phred-scaled quality 20 ("QUAL > 20") and read depth 2 ("DP > 2") using vcffilter from vcflib

473 (https://github.com/vcflib/vcflib). This allowed detecting variants that had reached high frequency

474 (min. 50 %) in a total of 229 samples representing abundant species in the experiment during (day

475 32) and after recovery from (day 48) the antibiotic pulse. Variants were annotated using SnpEff

476 4.3[62].

477

478 **Ecological analyses**

479

480 All analyses were performed in the R v3.6.1 environment[63]. The t-distributed stochastic neighbor

481 embedding (t-SNE) map for Extended Data Figure 1 was created using the Rtsne package[64] with the

482 options perplexity = 20 and theta = 0.5. Random forest models using community composition data

483 to classify the antibiotic or immigration treatments after the antibiotic pulse or following the recov-

484 ery period were generated using the randomForest package[65]. Before analyses, rare species were

485 removed based on > 80 % of values being zero, and the data was standardized by converting each

486 value into a Z-score (subtracting each sample's mean and dividing by the sample's standard devia-

487 tion). Random forest classification was performed using the function randomForest implementing

488 the Breiman's random forest algorithm, with the options importance = TRUE and proximities =

489 TRUE. Subsequently, permutation tests (1,000 permutations) were implemented using the function

490 rf.significance to test whether the models perform better than expected by chance. Following this,

491 the function train in the package caret[66] was used to systematically partition the data into training

492 and tests sets repeatedly using the leave-one-out cross-validation (LOOCV) approach to estimate

493 model performance (accuracy).

494

495 The influence of the experimental treatments on KL divergence relative to the pre-disturbance state

496 was investigated using generalized least squares models (gls) as implemented in the nlme package[67],

497 specifying a residual variance structure dependent on the antibiotic level. The stepAIC function in

498 the MASS package[68] was subsequently used to select the best model based on the Akaike infor-

499 mation criterion (AIC). The competitive fitness of species during the antibiotic pulse or the recov-

24

500   ery period was estimated as the logarithm of the final frequency relative to the starting frequency,

501   which can be directly derived from the replicator equation in evolutionary game theory. The strain

502   *Azospirillum brasilense* HAMBI 3172 was chosen to be the reference and its logarithm of the final

503   frequency relative to the starting frequency was subtracted from all other values. To control for

504   noise from the frequency changes of low-abundance species and to award more weight to species

505   with high abundance in at least one of the estimated time points, a pseudocount constituting 1 %

506   proportion was added to the species abundance data prior to computing competitive fitness. The

507   effect of the experimental treatments on species extinction probability was tested using the base R

508   function glm with the option family = "binomial".

509

510   To quantify the repeatability of ecological dynamics, we used the diversity dissimilarity index[33]:

511

$$\frac{\frac{D_{pooled}}{D_{mean}} - 1}{M - 1}$$

512

513   where D is a diversity index (either Shannon diversity or species richness computed using the vegan

514   package[69]), and M is the number of communities whose species compositions are compared (over

515   time). If the species compositions of replicates are identical, the diversity of the pooled community

516   is equal to the mean diversity, and the diversity dissimilarity index equals 0, and if the communities

517   have no species in common, the index equals 1.

518

519   **Evolutionary analyses**

520

521   We used minimal criteria to filter raw genomic variants from the downsampled variant data prior to

522   downstream analyses. First, we removed data for one species, HAMBI 403, which had a large num-

523   ber of variants (130,000) indicative of an incorrect reference genome. Second, there were peaks

524   above 80 % in variant frequency distributions across the communities. Such a high level of parallel-

525   ism suggests that the variants are either ancestral or systematic sequencing errors, and variants oc-

526   curring in over 80 % of the communities were therefore removed.

527

528   From this variant data set, we extracted nonsynonymous mutations and devised a threshold for re-

529   currence. Of all the coding genes in all the genomes, we drew mutations from a multinomial distri-

530   bution with replacement. If these 588 mutations were randomly distributed over the 58,220 coding

531   genes in the genomes, we would expect only five genes mutated in two or more populations. In total,

532   there were 1092 coding nonsynonymous mutations across 47 genes independently mutated in two

533   or more populations. Therefore, we focused on multi-hit genes which were independently mutated

534   in two or more populations. This set was used for the statistical analysis below, while a larger set

535   from genomic variant data prior to downsampling, and also including the known streptomycin re-

536   sistance gene *rpsL*, was used for Figure 6 to present the maximum amount of functionally annotated

537   potential targets of selection.

538

539   We used permutational analysis of variance (PERMANOVA)[70] to test whether the antibiotic level

540   or presence/absence of immigration affected the targets of mutation. Each community was scored

541   by the presence (1) or absence (0) of a nonsynonymous mutation in each of the multi-hit genes, and

542   these data were used to calculate the Euclidian distance between populations[71]. Before performing

543   PERMANOVA, its assumption of homogeneity of multivariate dispersions within treatments was

544   tested with the betadisper function in the vegan package that uses the PERMDISP2 procedure as

545   described previously[72]. The adonis function in the vegan package was then used to test the probabil-

546   ity that the observed distances could arise by chance by comparing them with random permutations

547   of the raw data[73].

Data availability

Raw sequence data (fastq files) has been deposited in the NCBI Sequence Read Archive (SRA) under the accession PRJNA632457. All code and pre-processed data needed to reproduce the downstream analyses and figures are available via GitHub: https://github.com/johannescairns/repeatable_dynamics (permanent doi: https://doi.org/10.5281/zenodo.3908935).

References

1. Smith, M.D., Knapp, A.K. & Collins, S.L. A framework for assessing ecosystem dynamics in response to chronic resource alterations induced by global change. *Ecology* **90**, 3279–3289 (2009).

2. Rockstrom, J., et al. A safe operating space for humanity. *Nature* **461**, 472–475 (2009).

3. Morley, V.J., Woods, R.J. & Read, A.F. Bystander selection for antimicrobial resistance: Implications for patient health. *Trends Microbiol* **27**, 864–877 (2019).

4. Vrancken, G., Gregory, A.C., Huys, G.R.B., Faust, K. & Raes, J. Synthetic ecology of the human gut microbiota. *Nat Rev Microbiol* **17**, 754–763 (2019).

5. Lässig, M., Mustonen, V. & Walczak, A.M. Predicting evolution. *Nat Ecol Evol* **1**, 77 (2017).

6. Robinson, J.I., et al. Metabolomic networks connect host-microbiome processes to human *Clostridioides difficile* infections. *J Clin Invest* **130**, 3792–3806 (2019).

7. Oh, S., Choi, D. & Cha, C.J. Ecological processes underpinning microbial community structure during exposure to subinhibitory level of triclosan. *Sci Rep* **9**, 4598 (2019).

573   8.   Zorner, P., Farmer, S. & Alibek, K. Quantifying crop rhizosphere microbiome ecology: The

574   next frontier in enhancing the commercial utility of agricultural microbes. *Ind Biotechnol (New*

575   *Rochelle N Y)* **14**, 116–119 (2018).

576   9.   Lozada-Gobilard, S., et al. Environmental filtering predicts plant-community trait distribution

577   and diversity: Kettle holes as models of meta-community systems. *Ecol Evol* **9**, 1898–1910

578   (2019).

579   10.   Li, J., et al. Shared molecular targets confer resistance over short and long evolutionary time-

580   scales. *Mol Biol Evol* **36**, 691–708 (2019).

581   11.   Vázquez-García, I., et al. Clonal heterogeneity influences the fate of new adaptive mutations.

582   *Cell Rep* **21**, 732–744 (2017).

583   12.   Illingworth, C.J.R., Parts, L., Schiffels, S., Liti, G. & Mustonen, V. Quantifying selection act-

584   ing on a complex trait using allele frequency time series data. *Mol Biol Evol* **29**, 1187–1197

585   (2012).

586   13.   Leibler, S. & Kussell, E. Individual histories and selection in heterogeneous populations. *Proc*

587   *Natl Acad Sci U S A* **107**, 13183–13188 (2010).

588   14.   Des Roches, S., et al. The ecological importance of intraspecific variation. *Nat Ecol Evol* **2**, 57–

589   64 (2018).

590   15.   Wistrand-Yuen, E., et al. Evolution of high-level resistance during low-level antibiotic expo-

591   sure. *Nat Commun* **9**, 1599 (2018).

592   16.   Schoener, T.W. The newest synthesis: Understanding the interplay of evolutionary and ecolog-

593   ical dynamics. *Science* **331**, 426–429 (2011).

594   17.   Scheuerl, T., et al. Bacterial adaptation is constrained in complex communities. *Nat Commun*

595   **11**, 754 (2020).

596   18. Roodgar, M., et al. Longitudinal linked read sequencing reveals ecological and evolutionary

597   responses of a human gut microbiome during antibiotic treatment. *bioRxiv* 2019.12.21.886093.

598   doi:https://doi.org/10.1101/2019.12.21.886093

599   19. Dethlefsen, L. & Relman, D.A. Incomplete recovery and individualized responses of the human

600   distal gut microbiota to repeated antibiotic perturbation. *Proc Natl Acad Sci U S A* **108**,

601   S1:4554–4561 (2011).

602   20. Palleja, A., et al. Recovery of gut microbiota of healthy adults following antibiotic exposure.

603   *Nat Microbiol* **3**, 1255–1265 (2018).

604   21. Jernberg, C., Lofmark, S., Edlund, C. & Jansson, J.K. Long-term ecological impacts of antibi-

605   otic administration on the human intestinal microbiota. *ISME J* **1**, 56–66 (2007).

606   22. Yassour, M., et al. Natural history of the infant gut microbiome and impact of antibiotic treat-

607   ment on bacterial strain diversity and stability. *Sci Transl Med* **8**, 343ra81 (2016).

608   23. Mack, I., et al. Antimicrobial resistance following azithromycin mass drug administration: Po-

609   tential surveillance strategies to assess public health impact. *Clin Infect Dis* **pii**, ciz893 (2019).

610   24. Tamburini, S., Shen, N., Wu, H.C. & Clemente, J.C. The microbiome in early life: Implications

611   for health outcomes. *Nat Med* **22**, 713–722 (2016).

612   25. Langdon, A., Crook, N. & Dantas, G. The effects of antibiotics on the microbiome throughout

613   development and alternative approaches for therapeutic modulation. *Genome Med* **8**, 39 (2016).

614   26. Brown, J.H. & Kodricbrown, A. Turnover rates in insular biogeography: Effect of immigration

615   on extinction. *Ecology* **58**, 445–449 (1977).

616   27. Patel, R. & DuPont, H.L. New approaches for bacteriotherapy: Prebiotics, new-generation pro-

617   biotics, and synbiotics. *Clin Infect Dis* **60**, S2:108–121 (2015).

618   28. Lawley, T.D., et al. Targeted restoration of the intestinal microbiota with a simple, defined bac-

619   teriotherapy resolves relapsing *Clostridium difficile* disease in mice. *PLoS Pathog* **8**, e1002995

620   (2012).

621 29. Ingrisch, J. & Bahn, M. Towards a comparable quantification of resilience. *Trends Ecol Evol*

622   **33**, 251–259 (2018).

623 30. Morton, J.T., et al. Establishing microbial composition measurement standards with reference

624   frames. *Nat Commun* **10**, 2719 (2019).

625 31. Trindade, S., Sousa, A. & Gordo, I. Antibiotic resistance and stress in the light of Fisher's mod-

626   el. *Evolution* **66**, 3815–3824 (2012).

627 32. Day, T., Huijben, V. & Read, A.F. Is selection relevant in the evolutionary emergence of drug

628   resistance? *Trends Microbiol* **23**, 126–133 (2015).

629 33. Lerner, J., et al. Chromosomal barcoding of *E. coli* populations reveals lineage diversity dy-

630   namics at high resolution. *bioRxiv* 571505. doi:https://doi.org/10.1101/571505

631 34. Springer, B., et al. Mechanisms of streptomycin resistance: Selection of mutations in the 16S

632   rRNA gene conferring resistance. *Antimicrob Agents Chemother* **45**, 2877–2884 (2001).

633 35. Nishimura, K., Hosaka, T., Tokuyama, S., Okamoto, S. & Ochi, K. Mutations in *rsmG*, encod-

634   ing a 16S rRNA methyltransferase, result in low-level streptomycin resistance and antibiotic

635   overproduction in *Streptomyces coelicolor* A3(2). *J Bacteriol* **189**, 3876–3883 (2007).

636 36. Macfarlane, E.L.A., Kwasnicka, A. & Hancock, R.E.W. Role of *Pseudomonas aeruginosa*

637   PhoP-phoQ in resistance to antimicrobial cationic peptides and aminoglycosides. *Microbiology*

638   **146**, Pt 10:2543–2554 (2000).

639 37. Girgis, H.S., Hottes, A.K. & Tavazoie, S. Genetic architecture of intrinsic antibiotic suscepti-

640   bility. *PLOS ONE* **4**, e5629 (2009).

641 38. Yongjuan Liu, X.C., Long Pan & Zhonggui Mao. Differential protein expression of a strepto-

642   mycin-resistant *Streptomyces albulus* mutant in high yield production of ε-poly-l-lysine: A pro-

643   teomics study. *RSC Adv* **9**, 24092 (2019).

644 39. Beardmore, R.E., et al. Drug-mediated metabolic tipping between antibiotic resistant states in a

645   mixed-species community. *Nat Ecol Evol* **2**, 1312–1320 (2018).

646 40. Perron, G.G., Gonzalez, A. & Buckling, A. The rate of environmental change drives adaptation

647   to an antibiotic sink. *J Evol Biol* **21**, 1724–1731 (2008).

648 41. Retel, C., et al. The feedback between selection and demography shapes genomic diversity dur-

649   ing coevolution. *Sci Adv* **5**, eaax0530 (2019).

650 42. Melnyk, A.H., Wong, A. & Kassen, R. The fitness costs of antibiotic resistance mutations. *Evol*

651   *Appl* **8**, 273–283 (2015).

652 43. Wein, T., et al. Carrying capacity and colonization dynamics of *Curvibacter* in the *Hydra* host

653   habitat. *Front Microbiol* **9**, 443 (2018).

654 44. Zhou, J., et al. Stochastic assembly leads to alternative communities with distinct functions in a

655   bioreactor microbial community. *mBio* **4**, e00584-12 (2013).

656 45. Lozupone, C.A., Stombaugh, J.I., Gordon, J.I., Jansson, J.K. & Knight, R. Diversity, stability

657   and resilience of the human gut microbiota. *Nature* **489**, 220–230 (2012).

658 46. Shade, A., et al. Fundamentals of microbial community resistance and resilience. *Front Micro-*

659   *biol* **3**, 417 (2012).

660 47. Waples, R.S., Beechie, T. & Pess, G.R. Evolutionary history, habitat disturbance regimes, and

661   anthropogenic changes: What do these mean for resilience of Pacific salmon populations? *Ecol*

662   *Soc* **14**, 3 (2009).

663 48. Johnstone, J.F., et al. Changing disturbance regimes, ecological memory, and forest resilience.

664   *Front Ecol Environ* **14**, 369–378 (2016).

665 49. Cairns, J., et al. Construction and characterization of synthetic bacterial community for experi-

666   mental ecology and evolution. *Front Genet* **9**, 312 (2018).

667 50. Datta, N., Hedges, R.W., Shaw, E.J., Sykes, R.B. & Richmond, M.H. Properties of an R factor

668   from *Pseudomonas aeruginosa*. *J Bacteriol* **108**, 1244–1249 (1971).

669 51. Cairns, J., et al. Ecology determines how low antibiotic concentration impacts community

670   composition and horizontal transfer of resistance genes. *Commun Biol* **1**, 35 (2018).

671   52. Zhang, J., Kobert, K., Flouri, T. & Stamatakis, A. PEAR: A fast and accurate Illumina Paired-
672   End reAd mergeR. *Bioinformatics* **30**, 614–620 (2014).

673   53. Martin, M. & Martin, M. Cutadapt removes adapter sequences from high-throughput sequenc-
674   ing reads. *Embnet.journal* **17**, 10–12 (2011).

675   54. Ewels, P., Magnusson, M., Lundin, S. & Kaller, M. MultiQC: Summarize analysis results for
676   multiple tools and samples in a single report. *Bioinformatics* **32**, 3047–3048 (2016).

677   55. Edgar, R.C. UPARSE: Highly accurate OTU sequences from microbial amplicon reads. *Nat*
678   *Methods* **10**, 996–998 (2013).

679   56. Rognes, T., Flouri, T., Nichols, B., Quince, C. & Mahe, F. VSEARCH: A versatile open source
680   tool for metagenomics. *PeerJ* **4**, e2584 (2016).

681   57. Edgar, R.C. Accuracy of microbial community diversity estimated by closed- and open-
682   reference OTUs. *PeerJ* **5**, e3889 (2017).

683   58. Langmead, B. & Salzberg, S.L. Fast gapped-read alignment with Bowtie 2. *Nat Methods* **9**,
684   357–359 (2012).

685   59. Li, H., et al. The Sequence Alignment/Map format and SAMtools. *Bioinformatics* **25**, 2078–
686   2079 (2009).

687   60. Quinlan, A.R. & Hall, I.M. BEDTools: A flexible suite of utilities for comparing genomic fea-
688   tures. *Bioinformatics* **26**, 841–842 (2010).

689   61. Garrison, E. & Gabor, M. Haplotype-based variant detection from short-read sequencing. *arXiv*
690   1207.3907 (2012).

691   62. Cingolani, P., et al. A program for annotating and predicting the effects of single nucleotide
692   polymorphisms, SnpEff: SNPs in the genome of *Drosophila melanogaster* strain w(1118); iso-
693   2; iso-3. *Fly* **6**, 80–92 (2012).

694   63. R Core Team. R: A language and environment for statistical computing. R Foundation for Sta-
695   tistical Computing, Vienna, Austria (2019). URL:https://www.R-project.org/.

696   64. Krijthe, J. Rtsne: T-distributed stochastic neighbor embedding using a Barnes-Hut imple-

697   mentation. R package version 0.15 (2015). URL:https://github.com/jkrijthe/Rtsne

698   65. Liaw, A. & Wiener, M. Classification and regression by randomForest. *R News* **2**, 18–22

699   (2002).

700   66. Kuhn, M., et al. caret: Classification and regression training. R package version 6.0-84 (2019).

701   URL:https://CRAN.R-project.org/package=caret

702   67. Pinheiro, J, Bates, D., DebRoy, S., Sarkar, D. & R Core Team. nlme: Linear and nonlinear

703   mixed effects models. R package version 3.1-142 (2019). URL:https://CRAN.R-

704   project.org/package=nlme

705   68. Venables, W.N. & Ripley, B.D. Modern applied statistics with S. Fourth Edition, Springer,

706   New York (2002).

707   69. Oksanen, J, et al. vegan: Community ecology package. R package version 2.5-6 (2019).

708   URL:https://CRAN.R-project.org/package=vegan

709   70. Zapala, M.A. & Schork, N.J. Multivariate regression analysis of distance matrices for testing

710   associations between gene expression patterns and related variables. *Proc Natl Acad Sci U S A*

711   **103**, 19430–19435 (2006).

712   71. Excoffier, L., Smouse, P.E. & Quattro, J.M. Analysis of molecular variance inferred from met-

713   ric distances among DNA haplotypes: Application to human mitochondrial DNA restriction da-

714   ta. *Genetics* **131**, 479–491 (1992).

715   72. Anderson, M.J. Distance-based tests for homogeneity of multivariate dispersions. *Biometrics*

716   **62**, 245–253 (2006).

717   73. Anderson, M.J. A new method for non-parametric multivariate analysis of variance. *Austral*

718   *Ecol* **26**, 32–46 (2001).

719

720

721

722

Acknowledgements

723

724

729

730 **Author contributions**

731

732 Design of serial passage experiment: TH, JC, LB. Performing serial passage experiment: RJ. Design

733 of data analysis: JC, VM, LB. Performing data analysis: JC. Interpreting results: JC, TH, LB, VM.

734 JC wrote the first manuscript draft, with contributions from all authors. All authors approve the fi-

735 nal version of the manuscript.

736

737 **Competing interests**

738

739 The authors state that they have no competing interests.

740

741

Figure legends

743

744 **Figure 1.** Experimental design. (A) Physical setup. A serial passage experiment was conducted
745 with a 34-species artificial community in deep 96-well plates. Initial key traits of community mem-
746 bers (intrinsic growth rate, represented by growth curve with yellow background, and intrinsic anti-
747 biotic susceptibility level, represented by growth curve in purple background) were measured sepa-
748 rately for individual isolates used to construct the community. (B) Layout of antibiotic pulse exper-
749 iment. The experiment consisted of serial propagation at 4-day (96 h) intervals for three 16-day
750 epochs: an acclimation period, an antibiotic pulse period with three different levels of pulse antibi-
751 otic disturbance together with an antibiotic-free control treatment, and a recovery period. To inves-
752 tigate the role of species immigration, the full experiment was performed without and with reintro-
753 ducing a small amount (1:500 cells relative to serial transfer inoculum) of the original community at
754 each transfer. Each unique treatment combination was replicated eight times. Samples (N = 192)
755 were collected for DNA extraction prior to the pulse (T0), after the pulse (T1) and after recovery
756 (T2) to track community composition (amplicon sequencing) and genomic evolution (metagenomic
757 sequencing).

758

759 **Figure 2.** Community dynamics during antibiotic pulse experiment. The figure depicts the frequen-
760 cies of abundant species across time in eight replicate communities for each unique treatment com-
761 bination indicated on the right (low, intermediate and high antibiotic levels correspond to 4, 16 and
762 128 μg ml^{-1} streptomycin, respectively). The shaded area shows the antibiotic pulse epoch, with
763 increasingly dark hue indicating increasing antibiotic level. The top four panels show the different
764 antibiotic levels for the immigration-free treatment and the bottom four panels for the immigration
765 treatment. The *y*-axis has been square root transformed and scaled 0–1 to allow visual discernment
766 of less abundant species. "Others" denotes rare taxa that fail to reach a frequency of 5 % in at least
767 one community and time point. In total, 190 experimental samples are included in the figure togeth-
768 er with one stock community sample to represent initial species composition for all communities.
769 For two communities, adequate amplicon sequence data could not be recovered for day 48.
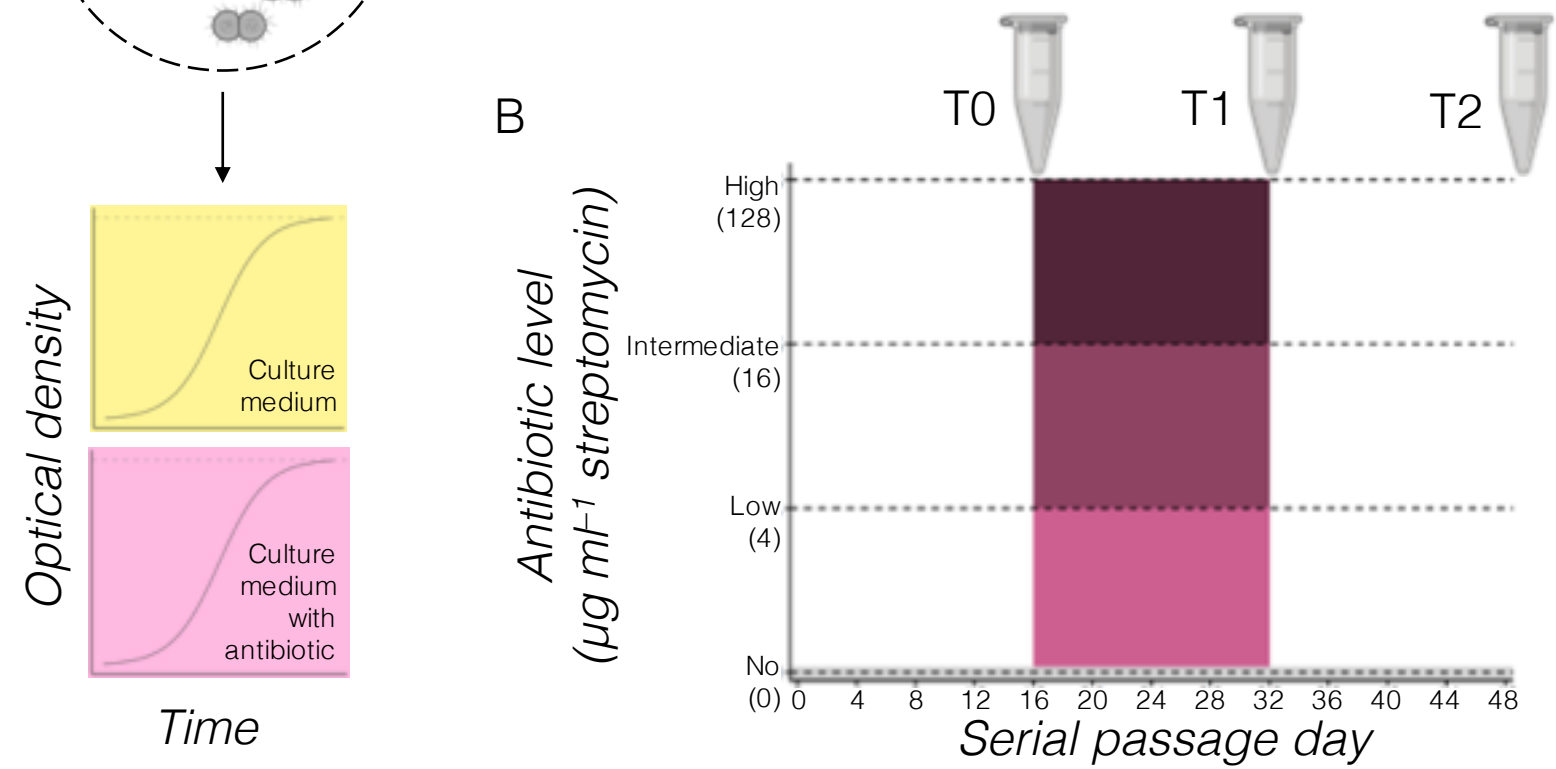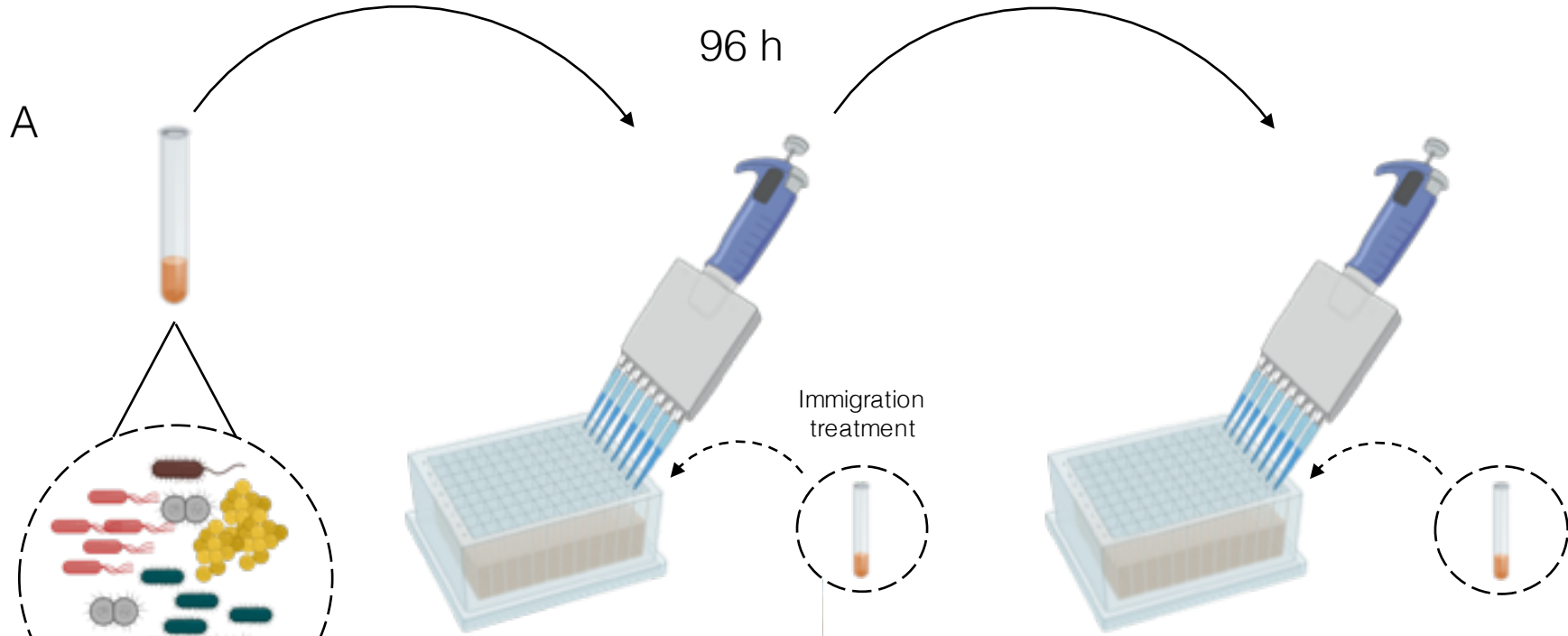
770

771 **Figure 3.** Community response to antibiotic perturbation. (A) Shannon diversity at the end of the
772 antibiotic pulse (N = 64). (B) Ecological resilience without (left) and with (right) species immigra-
773 tion (N = 190). Resilience has been quantified for each community separately as the Kullback-
774 Leibler (KL) divergence of community composition over time after the disturbance relative to the
775 pre-disturbance state. In both panels, the data for the respective metric (Shannon diversity or KL
776 divergence, both computed from species composition data) is displayed by a box and whiskers plot
777 overlaid by raw data points. The lower and upper hinges of the box and whiskers plot correspond to
778 the 25th and 75th percentiles, while the lower and upper and whiskers extend from the hinge to the
779 smallest or largest value, respectively (max. 1.5 × interquartile range from hinge). Low, intermedi-
780 ate and high antibiotic levels correspond to 4, 16 and 128 μg ml^{-1} streptomycin, respectively.

781

782 **Figure 4.** Competitive fitness of species in replicate communities (N = 8) during and after recovery
783 from intermediate-level antibiotic pulse (16 μg ml^{-1} streptomycin) in the absence of immigration
784 (mean indicated by dashed line). The figure illustrates the repeatability of the species response be-
785 tween replicate communities and the inverse response for multiple species during the perturbation
786 (top panel) versus recovery (bottom panel) phases. The competitive fitness of species is estimated

787 as the logarithm of the final frequency relative to the starting frequency, derived from the replicator
788 equation in evolutionary game theory. Data for replicate 7 is missing from the panel below because
789 of inadequate amplicon sequence data for one community sample (final time point).
790

791 **Figure 5.** Repeatability of community trajectories, assessed using the diversity dissimilarity index
792 (± bootstrapped standard error; N = 190) where zero indicates perfect identity and one complete
793 dissimilarity between replicate communities. Repeatability is shown separately for Shannon diversi-
794 ty (top), which gives more weight to abundant species, and species richness (bottom), which gives
795 equal weight to all species. The antibiotic pulse epoch is indicated by grey shade. Low, intermediate
796 and high antibiotic levels correspond to 4, 16 and 128 μg ml^{-1} streptomycin, respectively. The di-
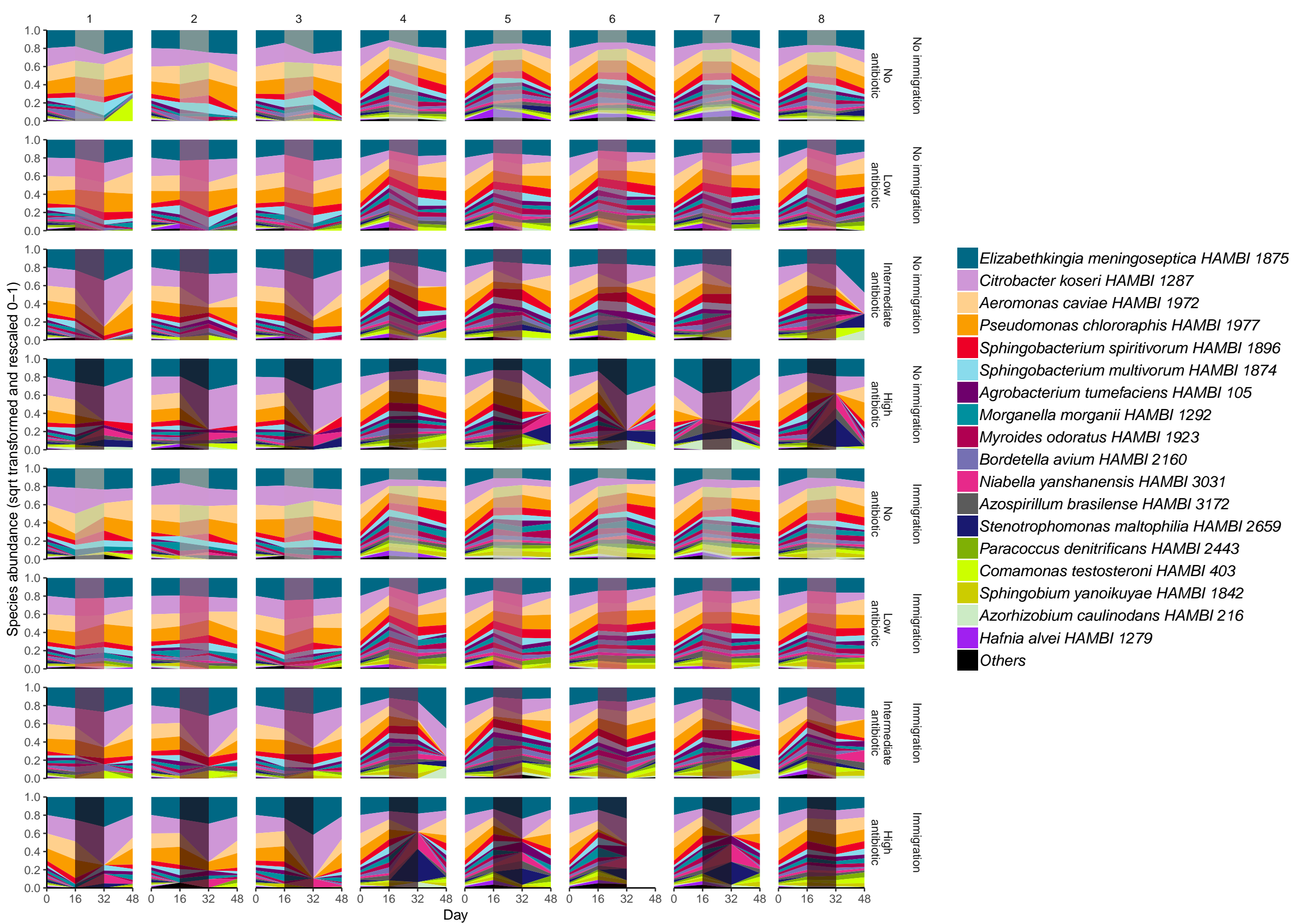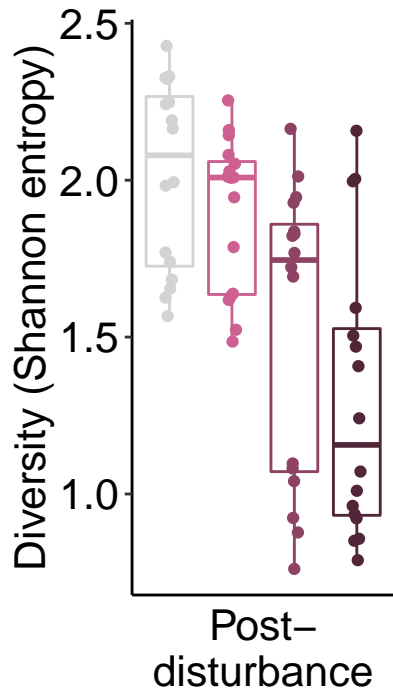797 versity dissimilarity index has been computed from species compositional data.
798

799 **Figure 6.** Targets of adaptive mutations reaching high frequencies (> 0.3 to fixation) in high-
800 abundance species during or after recovery from antibiotic pulse. The same mutations were mostly
801 observed in both time points when the species was detectable (i.e. mutation not lost during recov-
802 ery). The heat map shows functionally annotated targets of recurrent nonsynonymous mutations, as
803 well as the known streptomycin resistance gene *rpsL* which is only mutated in a single community.
804 Since the genomic variants were recovered from deep sequencing data, they could only be con-
805 firmed for a subset of the three sequenced replicates and experimental treatments owing to differen-
806 tial abundance of species and volume of sequence data. Color coding is used to indicate the number
807 of the replicates where a genomic target of interest was mutated relative to the number for which
808 genomic variant data could be recovered in a particular experimental treatment.
809

A

96 h

B

Immigration treatment

T0   T1   T2

Optical density

Culture medium

Culture medium with antibiotic

Time

Antibiotic level (µg ml⁻¹ streptomycin)

High (128)

Intermediate (16)

Low (4)

No (0)

Serial passage day

0   4   8   12 16 20 24 28 32 36 40 44 48

Species abundance (sqrt transformed and rescaled 0–1) plotted against Day (0, 16, 32, 48) across treatment panels. Columns labeled 1–8. Rows grouped by immigration status (No immigration / Immigration) and antibiotic level (No antibiotic, Low antibiotic, Intermediate antibiotic, High antibiotic).

Legend:
- *Elizabethkingia meningoseptica HAMBI 1875*
- *Citrobacter koseri HAMBI 1287*
- *Aeromonas caviae HAMBI 1972*
- *Pseudomonas chlororaphis HAMBI 1977*
- *Sphingobacterium spiritivorum HAMBI 1896*
- *Sphingobacterium multivorum HAMBI 1874*
- *Agrobacterium tumefaciens HAMBI 105*
- *Morganella morganii HAMBI 1292*
- *Myroides odoratus HAMBI 1923*
- *Bordetella avium HAMBI 2160*
- *Niabella yanshanensis HAMBI 3031*
- *Azospirillum brasilense HAMBI 3172*
- *Stenotrophomonas maltophilia HAMBI 2659*
- *Paracoccus denitrificans HAMBI 2443*
- *Comamonas testosteroni HAMBI 403*
- *Sphingobium yanoikuyae HAMBI 1842*
- *Azorhizobium caulinodans HAMBI 216*
- *Hafnia alvei HAMBI 1279*
- *Others*